Supporting Information for Publication

Identification of inhibitors of SARS-CoV-2 3CL-Pro enzymatic activity using a small molecule in-vitro repurposing screen

Maria Kuzikov[1*], Elisa Costanzi[2], Jeanette Reinshagen[1], Francesca Esposito[3], Laura Vangeel[4], Markus Wolf[1], Bernhard Ellinger[1], Carsten Claussen[1], Gerd Geisslinger[1,11], Angela Corona[3], Daniela Iaconis[5], Carmine Talarico[5], Candida Manelfi[5], Rolando Cannalire[6], Giulia Rossetti[7], Jonas Gossen[7], Simone Albani[7], Francesco Musiani[8], Katja Herzog[9], Yang Ye[10], Barbara Giabbai[2], Nicola Demitri[2], Dirk Jochmans[4], Steven De Jonghe[4], Jasper Rymenants[4], Vincenzo Summa[6], Enzo Tramontano[3], Andrea R. Beccari[5], Pieter Leyssen[4], Paola Storici[2], Johan Neyts[4], Philip Gribbon[1] and Andrea Zaliani[1]

1) Fraunhofer Institute for Translational Medicine and Pharmacology (ITMP) and Fraunhofer Cluster of Excellence for Immune mediated diseases (CIMD), Schnackenburgallee 114, 22525 Hamburg, and Theodor Stern Kai 7, 60590 Frankfurt, Germany

2) Elettra-Sincrotrone Trieste S.C.p.A., SS 14 - km 163, 5 in AREA Science Park 34149 Basovizza, Trieste, Italy

3) Dipartimento di Scienze della vita e dell'ambiente, Cittadella Universitaria di Monserrato, SS-554, Monserrato, Cagliari, Italy

4) KU Leuven, Department of Microbiology, Immunology and Transplantation, Rega Institute for Medical Research, Laboratory of Virology and Chemotherapy, Herestraat 49 - box 1043, 3000- Leuven, Belgium

5) Dompé Farmaceutici SpA, via Campo di Pile, 67100 L'Aquila, Italy

6) Department of Pharmacy, University of Naples Federico II, Via D. Montesano, 49, 80131 Naples, Italy

7) Institute of Neuroscience and Medicine (INM-9)/Institute for Advanced Simulation (IAS-5) and Jülich Supercomputing Centre (JSC) Forschungszentrum Jülich D-52425 Jülich, Germany

8) Laboratory of Bioinorganic Chemistry, Department of Pharmacy and Biotechnology, University of Bologna, Bologna, Italy.

9) EU-OPENSCREEN ERIC, Robert-Rössle-Straße 10, 13125 Berlin, Germany

10) University of Chinese Academy of Sciences, Beijing, 100049, China

11) Institute of Clinical Pharmacology, Goethe-University, Theodor Stern Kai 7, 60590 Frankfurt, Germany

*corresponding author: Maria Kuzikov, maria.kuzikov@itmp.fraunhofer.de

Contents

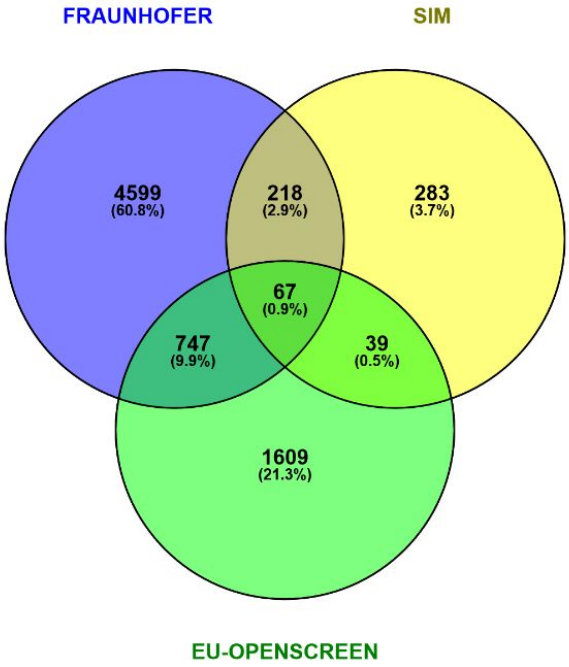

Figure S-1. Venn diagram showing overlap across the three compound collections (EU-OPENSCREEN, DOMPE Safe in Man (SIM) and EU-OPENSCREEN Bioactives) which composed the screened set. Percentages are relative to the total of 8702 compounds.

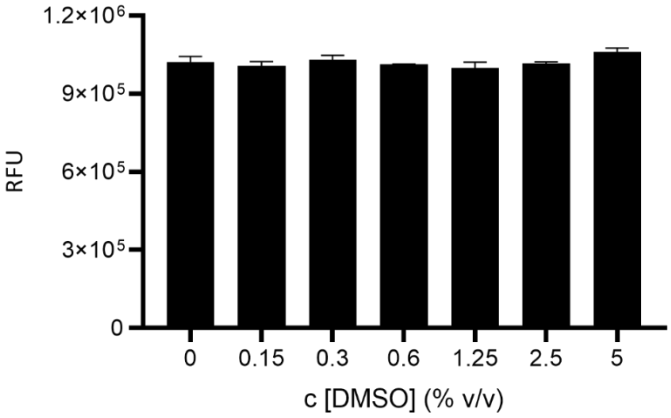

Figure S-2. Fluorescence intensity versus DMSO concentration % vol/vol. Assay conditions as per SARS-CoV-2 3CL-Pro primary screen.

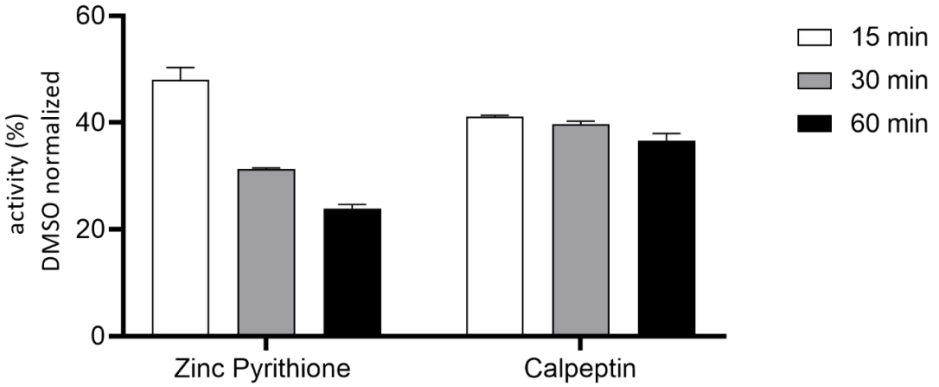

Figure S-3. Effects of compound pre-incubation times with SARS-CoV-2 3CL-Pro, on inhibitory activity of zinc pyrithione and calpeptin. Data are expressed as measured enzyme activity (%) in the presence of compound, normalised to corresponding DMSO control (100 % activity). Enzyme and substrate concentrations as per primary assay (no DTT). Pre-incubation temperature was 25 °C, with plates read at 15 minutes post substrate addition.

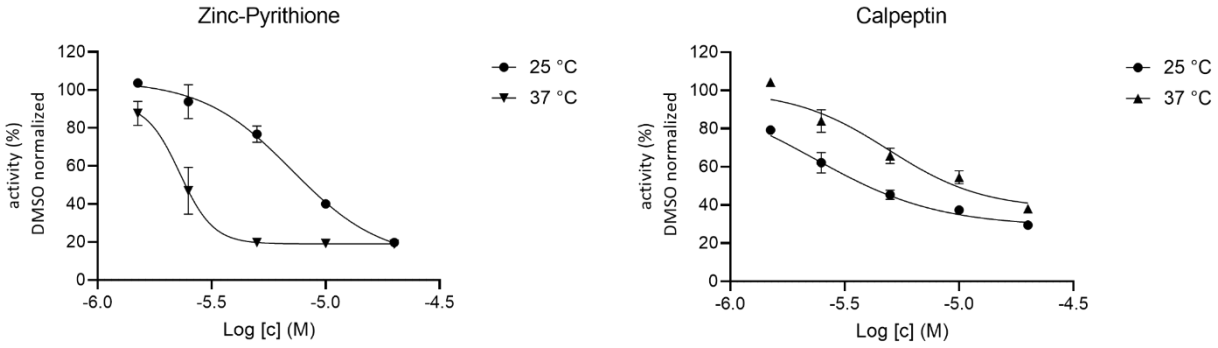

Figure S-4. Effects of temperature during the pre-incubation stage of reference compounds with SARS-CoV-2 3CL-Pro enzyme. Zinc pyrithione IC_{50}'s = 7.1 and 2.3 µM at 37 °C and 25°C, respectively. Calpeptin IC_{50}'s = 2.3 and 4.9 µM at 37 °C and 25°C, respectively. Assay buffer, enzyme, substrate and timings as per primary assay. SARS-COV-2 3CL-Pro incubated with 0.5 v/v % DMSO represents 100 % activity.

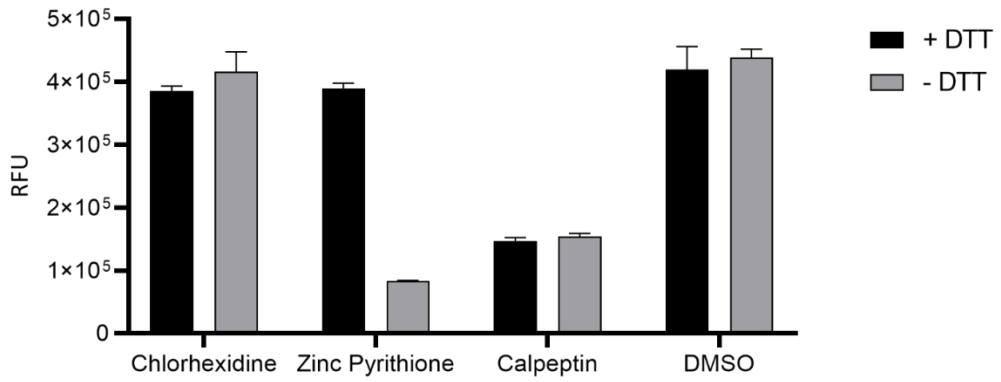

Figure S-5. Dependence of inhibition of proposed SARS-CoV-2 3CL-Pro inhibitors on DTT (at 0 or 1mM). Test compound concentration 20 µM. Enzyme, substrate and timing conditions as per primary screen

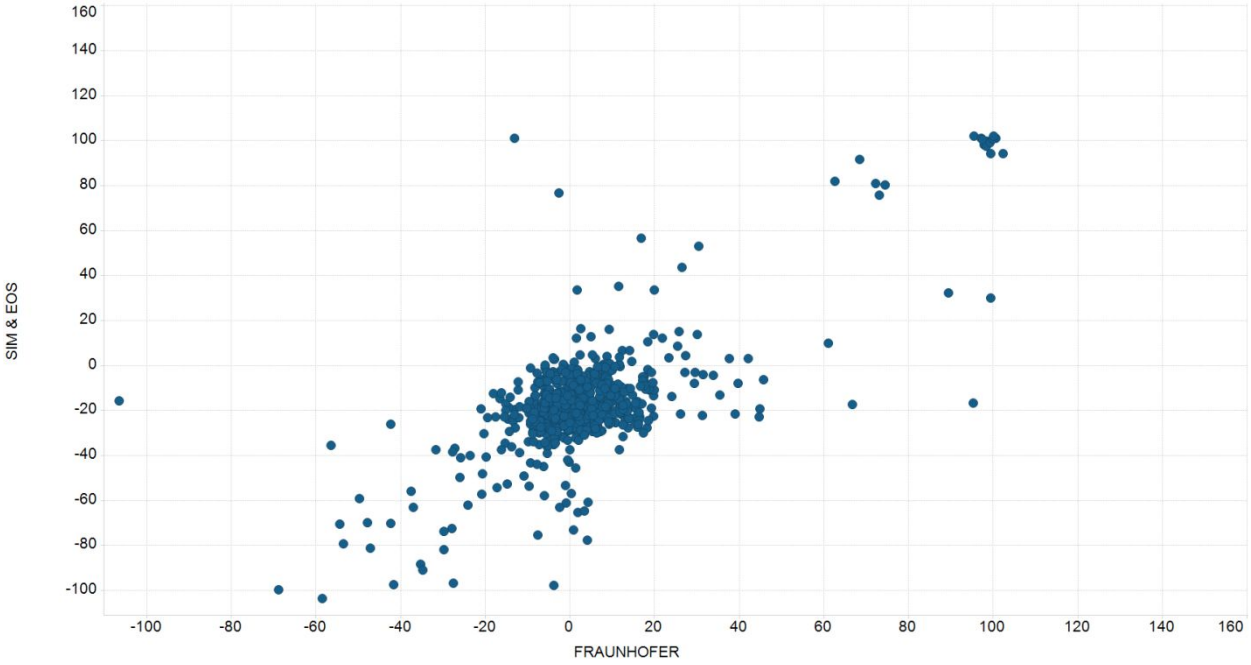

Figure S-6. Primary screen - comparison of compounds duplicated in different collections. Primary Screening Inhibition (%) of 3CL-Pro collected by compounds in Fraunhofer repurposing collection (x-axis) versus structurally identical compounds found in EU-OS or DOMPE collections. Data from compounds doubly or triply represented in the libraries (see Figure S1) Linear regression fit R^2= 0.78.

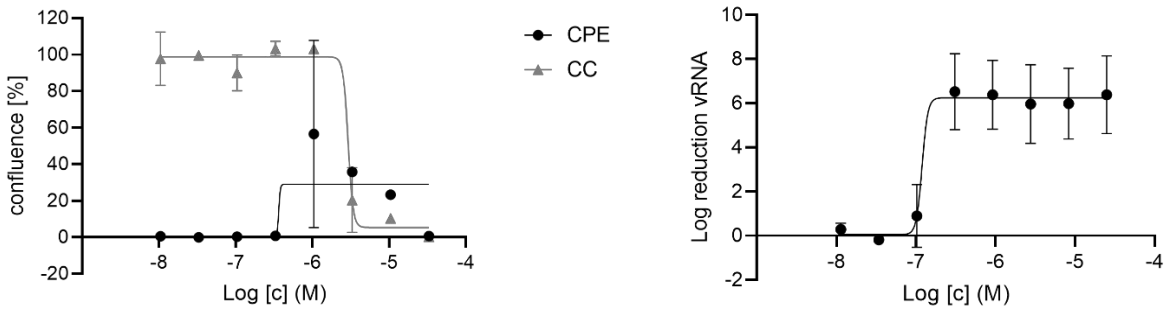

Figure S-7. MG-132, inhibition of virus induced cytopathic effect in Vero-E6 cells (IC_{50} = 0.36 µM), including the cytotoxicity (CC_{50}= 2.9 µM) (left) versus inhibition of viral replication in Vero-E6 (IC_{50} = 0.12 µM) (assessed by qPCR) (right)

Supplementary Modelling

Due to the thiol group and thio-ketonic group can affect the binding mode of thioguanosine, explaining its reactivity, the tautomeric distributions were calculated, using DFT implemented in Wavefunction Spartan '18, at B3LYP/AUG-cc-pVTZ basis set. Tautomer distribution results showed a clear separation in terms of Boltzmann weights for the six generated tautomers (Fig S7), highlighting the prevalence of the thioguanosine_T4 form with respect to the thio-ketonic group form thioguanosine_T3.

In particular, the molecular mechanically optimized equilibrium geometry with DFT, using the augmented representations of B3LYP/cc-pVTZ polarization basis sets (AUG-cc-pVTZ) was evaluated [Thom H. Dunning Jr. Gaussian basis sets for use in correlated molecular calculations. I. The atoms boron through neon and hydrogen. *The Journal of Chemical Physics* 90:2, 1007-1023] .

To avoid conformational bias that could occur given the presence of the b-D-ribofuranosyl group, the nitrogen atom at position 6 was methylated.

A geometrical docking method was performed with LiGen™, proprietary software developed by Dompé, for the identification of the best binding mode.[Error! Bookmark not defined.,Error! Bookmark not defined.] In particular, the docking search was focused within the 3CL-Pro binding site, by defining the free points within a three-dimensional grid, which include the entire binding site. The free points will be used by the docking procedures to define the pharmacophoric key points. The docking software follows a specific workflow during which three docking scores are computed: first, the Pacman Score (PS) estimates a geometric fitting score to evaluate the interaction between a ligand arrangement and the pocket, based on shape and volume complementarity. Then, the Chemical Score (CS), which encodes for the ligand binding interaction energy and is calculated by using an in-house developed scoring function[Error! Bookmark not defined.]. A rigid body minimization of the docked ligand within the binding site is the last step, at the end of which a third score called the Optimized Chemical Score (Csopt) is evaluated.

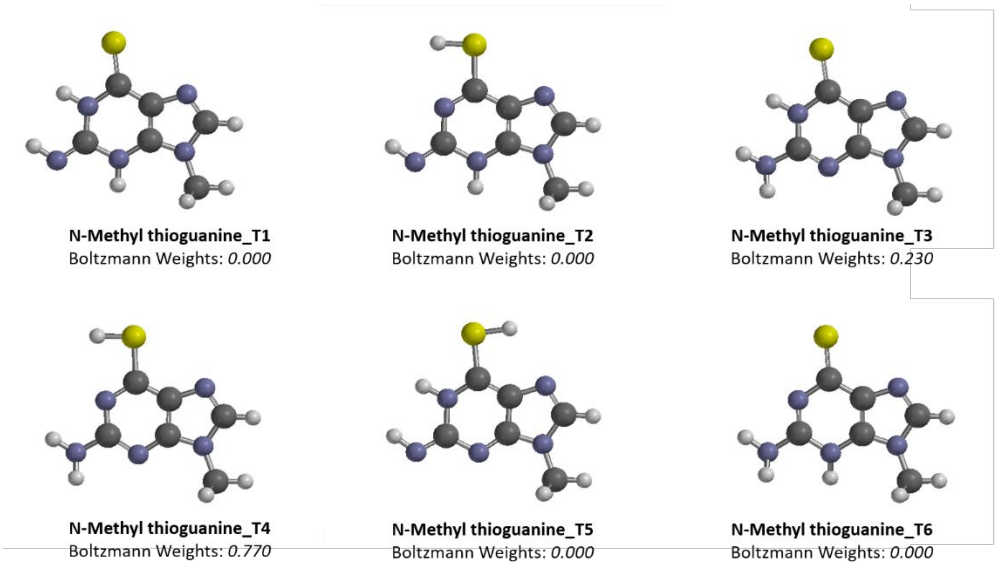

Figure S-8. The six optimized structures of N-methyl thioguanine (used as surrogate thioguanosine, as noted in the text) tautomers at B3LYP/AUG-cc-pVTZ basis set.

Table S-1. Primary screen quality control. Z prime versus plate ID.

Plate Id	Z Prime
ESP0026074	0.89
ESP0026075	0.86
ESP0026076	0.87
ESP0026077	0.83
ESP0026078	0.91
ESP0026079	0.82
ESP0026080	0.85
ESP0026081	0.84
ESP0026082	0.87
ESP0026083	0.86
ESP0026084	0.87
ESP0026085	0.88
ESP0026086	0.86
ESP0026087	0.88
ESP0026088	0.87
ESP0026089	0.87
ESP0026154	0.69
ESP0026155	0.76
ESP0026478	0.89
ESP0026479	0.91
ESP0026480	0.86
ESP0026481	0.87
ESP0026482	0.91
ESP0026483	0.9
ESP0026484	0.76

Table S-2. Primary screening results.
(https://www.ebi.ac.uk/chembl/document_report_card/CHEMBL4495564)

Table S-3. Hit confirmation and profiling data summary

SuppTable3.xlsx

Table S-4. Data collection and refinement statistics. Statistics for the highest-resolution shell are shown in parentheses.

Mpro-myricetin	
Data collection	
PDB ID	7B3E
Space group	P2(1)2(1)2(1)
Unit Cell Parameters	
a, b, c (Å)	67.834, 101.104, 103.559
α, β, γ (°)	90, 90, 90
Wavelength (Å)	0.9717
Resolution (Å)	103.56-1.77 (1.87-1.77)
Number of unique reflections	70132 (3958)
R_{merge}	0.110 (1.585)
R_{meas}	0.117 (1.681)
R_{pim}	0.039 (0.554)
<I/σ(I)>	11.3 (1.5)
$CC^{1/2}$	0.998 (0.570)
Completeness (%)	100 (100)
Multiplicity	8.8 (9.0)
Refinement	
Resolution (Å)	49.48-1.77
Number of reflections	70049
Number Reflections (R-Free)	3411
R_{work}/R_{free} (%)	17.12 / 20.38
r.m.s. deviations	
bond length (Å)	0.008
bond angles (°)	0.927
Ramachandran plot	
favored (%)	98.16
allowed (%)	1.84
outliers (%)	0.00